Dynamical Relativistic Effects in Quasielastic $1p$-Shell Proton Knockout from ^{16}O

J. Gao,[17] B. D. Anderson,[13] K. A. Aniol,[2] L. Auerbach,[29] F. T. Baker,[7] J. Berthot,[1] W. Bertozzi,[17] P.-Y. Bertin,[1] L. Bimbot,[22] W. U. Boeglin,[5] E. J. Brash,[24] V. Breton,[1] H. Breuer,[16] E. Burtin,[26] J. R. Calarco,[18] L. Cardman,[30] G. D. Cates,[23] C. Cavata,[26] C. C. Chang,[16] J.-P. Chen,[30] E. Cisbani,[12] D. S. Dale,[14] R. De Leo,[10] A. Deur,[1] B. Diederich,[21] P. Djawotho,[33] J. Domingo,[30] B. Doyle,[14] J.-E. Ducret,[26] M. B. Epstein,[2] L. A. Ewell,[16] J. M. Finn,[33] K. G. Fissum,[17] H. Fonvieille,[1] B. Frois,[26] S. Frullani,[12] F. Garibaldi,[12] A. Gasparian,[8,14] S. Gilad,[17] R. Gilman,[25,30] A. Glamazdin,[15] C. Glashausser,[25] J. Gomez,[30] V. Gorbenko,[15] T. Gorringe,[14] K. Griffioen,[33] F. W. Hersman,[18] R. Holmes,[28] M. Holtrop,[18] N. d'Hose,[26] C. Howell,[4] G. M. Huber,[24] C. E. Hyde-Wright,[21] M. Iodice,[12] C. W. de Jager,[30] S. Jaminion,[1] M. K. Jones,[33] K. Joo,[32] C. Jutier,[1,21] W. Kahl,[28] S. Kato,[34] J. J. Kelly,[16] S. Kerhoas,[26] M. Khandaker,[19] M. Khayat,[13] K. Kino,[31] W. Korsh,[14] L. Kramer,[5] K. S. Kumar,[23] G. Kumbartzki,[25] G. Laveissière,[1] A. Leone,[11] J. J. LeRose,[30] L. Levchuk,[15] M. Liang,[30] R. A. Lindgren,[32] N. Liyanage,[17] G. J. Lolos,[24] R. W. Lourie,[27] R. Madey,[8,13,30] K. Maeda,[31] S. Malov,[25] D. M. Manley,[13] D. J. Margaziotis,[2] P. Markowitz,[5] J. Martino,[26] J. S. McCarthy,[32] K. McCormick,[21] J. McIntyre,[25] R. L. J. van der Meer,[24] Z.-E. Meziani,[29] R. Michaels,[30] J. Mougey,[3] S. Nanda,[30] D. Neyret,[26] E. A. J. M. Offermann,[30] Z. Papandreou,[24] C. F. Perdrisat,[33] R. Perrino,[11] G. G. Petratos,[13] S. Platchkov,[26] R. Pomatsalyuk,[15] D. L. Prout,[13] V. A. Punjabi,[19] T. Pussieux,[26] G. Quéméner,[33] R. D. Ransome,[25] O. Ravel,[1] Y. Roblin,[1] R. Roche,[6] D. Rowntree,[17] G. A. Rutledge,[33] P. M. Rutt,[30] A. Saha,[30] T. Saito,[31] A. J. Sarty,[6] A. Serdarevic-Offermann,[24] T. P. Smith,[18] A. Soldi,[20] P. Sorokin,[15] P. Souder,[28] R. Suleiman,[13] J. A. Templon,[7] T. Terasawa,[31] L. Todor,[21] H. Tsubota,[31] H. Ueno,[34] P. E. Ulmer,[21] G. M. Urciuoli,[12] P. Vernin,[26] S. van Verst,[17] B. Vlahovic,[20] H. Voskanyan,[35] J. W. Watson,[13] L. B. Weinstein,[21] K. Wijesooriya,[33] R. Wilson,[9] B. Wojtsekhowski,[30] D. G. Zainea,[24] V. Zeps,[14] J. Zhao,[17] and Z.-L. Zhou[17]

(The Jefferson Lab Hall A Collaboration)

[1]*Université Blaise Pascal/IN2P3, F-63177 Aubière, France*
[2]*California State University, Los Angeles, California 90032*
[3]*Institut des Sciences Nucléaires, F-38026 Grenoble, France*
[4]*Duke University, Durham, North Carolina 27706*
[5]*Florida International University, Miami, Florida 33199*
[6]*Florida State University, Tallahassee, Florida 32306*
[7]*University of Georgia, Athens, Georgia 30602*
[8]*Hampton University, Hampton, Virginia 23668*
[9]*Harvard University, Cambridge, Massachusetts 02138*
[10]*INFN, Sezione di Bari and University of Bari, I-70126 Bari, Italy*
[11]*INFN, Sezione di Lecce, I-73100 Lecce, Italy*
[12]*INFN, Sezione Sanitá and Istituto Superiore di Sanitá, Laboratorio di Fisica, I-00161 Rome, Italy*
[13]*Kent State University, Kent, Ohio 44242*
[14]*University of Kentucky, Lexington, Kentucky 40506*
[15]*Kharkov Institute of Physics and Technology, Kharkov 310108, Ukraine*
[16]*University of Maryland, College Park, Maryland 20742*
[17]*Massachusetts Institute of Technology, Cambridge, Massachusetts 02139*
[18]*University of New Hampshire, Durham, New Hampshire 03824*
[19]*Norfolk State University, Norfolk, Virginia 23504*
[20]*North Carolina Central University, Durham, North Carolina 27707*
[21]*Old Dominion University, Norfolk, Virginia 23529*
[22]*Institut de Physique Nucléaire, F-91406 Orsay, France*
[23]*Princeton University, Princeton, New Jersey 08544*
[24]*University of Regina, Regina, Saskatchewan, Canada S4S 0A2*
[25]*Rutgers, The State University of New Jersey, Piscataway, New Jersey 08854*
[26]*CEA Saclay, F-91191 Gif-sur-Yvette, France*
[27]*State University of New York at Stony Brook, Stony Brook, New York 11794*
[28]*Syracuse University, Syracuse, New York 13244*
[29]*Temple University, Philadelphia, Pennsylvania 19122*
[30]*Thomas Jefferson National Accelerator Facility, Newport News, Virginia 23606*
[31]*Tohoku University, Sendai 980, Japan*
[32]*University of Virginia, Charlottesville, Virginia 22901*
[33]*College of William and Mary, Williamsburg, Virginia 23187*
[34]*Yamagata University, Yamagata 990, Japan*
[35]*Yerevan Physics Institute, Yerevan 375036, Armenia*

(Received 28 September 1999)

We have measured the cross section for quasielastic $1p$-shell proton knockout in the $^{16}O(e,e'p)$ reaction at $\omega = 0.439$ GeV and $Q^2 = 0.8$ (GeV$/c)^2$ for missing momentum $P_{\rm miss} \leq 355$ MeV$/c$. We have extracted the response functions R_{L+TT}, R_T, R_{LT}, and the left-right asymmetry, A_{LT}, for the $1p_{1/2}$ and the $1p_{3/2}$ states. The data are well described by relativistic distorted wave impulse approximation calculations. At large $P_{\rm miss}$, the structure observed in A_{LT} indicates the existence of dynamical relativistic effects.

PACS numbers: 25.30.Fj, 24.70.+s, 27.20.+n

Electron scattering is a powerful probe of the nuclear electromagnetic response [1,2]. Exclusive and semiexclusive proton knockout reactions, $(e,e'p)$, have long been used to study single-nucleon aspects of nuclear structure and to search for non-nucleonic degrees of freedom. At high four-momentum transfer squared [3], Q^2, quasielastic $(e,e'p)$ is expected to be dominated by single-body interactions, hence distorted wave impulse approximation (DWIA) calculations should be more accurate than at low Q^2. Calculations [4–7] indicate that in $^{16}O(e,e'p)$ the longitudinal-transverse interference response function [8], R_{LT}, and the left-right asymmetry, A_{LT}, are sensitive to dynamical enhancement of the distorted lower components of the Dirac spinors with respect to undistorted (free) spinors. The calculations predict that proper inclusion of these dynamical relativistic effects is needed to reproduce both A_{LT} and R_{LT}. We report structure in A_{LT} at large $P_{\rm miss}$ that shows for the first time clear evidence of the existence of dynamical relativistic effects in electromagnetic reactions.

$^{16}O(e,e'p)$ $1p$-shell proton knockout experiments have been performed at Saclay [9,10], NIKHEF [11,12], and Mainz [13] at low Q^2 [less than 0.4 (GeV$/c)^2$] in various kinematics. These experiments measured the cross section as a function of missing momentum and have extracted spectroscopic factors by comparing data to DWIA calculations. The published spectroscopic factors were between 0.5 and 0.7, but Kelly [2] showed that the data of Blomqvist *et al.* [13] suggest a significantly smaller normalization factor. Chinitz *et al.* [9] and Spaltro *et al.* [12] also extracted R_{LT}, the longitudinal-transverse interference response function, at $Q^2 = 0.3$ (GeV$/c)^2$ and 0.2 (GeV$/c)^2$, respectively. Their measurements of proton knockout from the $1p_{1/2}$ state agree, but their $1p_{3/2}$-state measurements disagree dramatically. DWIA calculations [7] are consistent with the data of Chinitz *et al.* [9].

This paper reports the results [14] of the first experiment [15] in Jefferson Lab Hall A [16]. In this experiment, we measured the $^{16}O(e,e'p)$ reaction cross section in quasielastic kinematics ($\omega = Q^2/2m_p$) at $Q^2 = 0.8$ (GeV$/c)^2$ and $\omega = 0.439$ GeV for $P_{\rm miss} <$ 355 MeV$/c$. We separated the response functions R_{L+TT}, R_T, and R_{LT}, and extracted A_{LT} for $1p$-shell proton knockout.

The 100% duty factor beam current of typically 70 μA was incident on a waterfall target with three foils, each about 130 mg/cm^2 thick along the beam line [17]. We used the two Hall A High Resolution Spectrometers [16] to detect the outgoing particles. We studied the spectrometer optical properties and acceptances both before and during the experiment. The angle of any tracked particle was determined to 0.3 mrad and its absolute momentum was measured with an accuracy $\frac{\delta p}{p} = 1.5 \times 10^{-3}$ [18–21].

The hydrogen in the H_2O target greatly simplified our normalizations and calibrations. We monitored the luminosity by continuously measuring the elastic $^1H(e,e)$ cross section. We used $^1H(e,ep)$ to determine the momentum transfer $|\vec{q}|$ absolutely to an accuracy of 1.5×10^{-3} and to reproduce this momentum transfer at each beam energy to a fractional accuracy of 1.5×10^{-4}.

We measured the cross section at fixed $|\vec{q}| =$ 992 MeV$/c$ at three beam energies (corresponding to three virtual photon polarizations) to separate the response functions and understand our systematic uncertainties (see Table I). The angles $\theta_{pq} = 0°$, $\pm 2.5°$, $\pm 8°$, $\pm 16°$, and $\pm 20°$ correspond to central missing momenta of 53, 60, 148, 280, and 345 MeV$/c$, respectively. Note that, at $\theta_{pq} = 0°$, we had to remove events with $P_{\rm miss} <$ 45 MeV$/c$ to eliminate contamination from $^1H(e,ep)$.

For $\theta_{pq} = \pm 8°$, the values of R_{LT} and A_{LT} extracted at $E_{\rm beam} = 2.4$ GeV agree with those extracted at $E_{\rm beam} =$ 1.6 GeV within 1 standard deviation. The overall systematic uncertainty in the cross-section measurements is about 5%. This uncertainty is dominated by the uncertainty in the $^1H(e,e)$ cross section to which the data were normalized [22]. We also studied the effect of the finite acceptance of the spectrometers on the cross sections. The difference between the cross sections averaged over the spectrometer acceptances and calculated for a small region of the central kinematics was approximately 1%.

We radiatively corrected the cross section using a modified version of the code RADCOR [23]. The missing energy resolution is 0.9 MeV FWHM, which does not allow us to resolve the $(2s_{1/2}, 1d_{5/2})$ doublet located at $E_{\rm miss} =$ 17.4 MeV from the $1p_{3/2}$ state (at $E_{\rm miss} = 18.4$ MeV).

TABLE I. Experimental kinematics.

$E_{\rm beam}$ (GeV)	θ_e (°)	θ_{pq} (°)
0.843	100.7	0, 8, 16
1.643	37.2	0, $\pm$8
2.442	23.4	0, $\pm$2.5, $\pm$8, $\pm$16, $\pm$20

The strength of this doublet was estimated using the spectroscopic factors obtained by Leuschner *et al.* [11] to be approximately 5% of the $1p_{3/2}$ strength for this kinematical region. It was not subtracted from the cross section for the $1p_{3/2}$ state.

The first relativistic calculations for $(e,e'p)$ were performed by Picklesimer and Van Orden [4,5]. We compared out data to more recent calculations by Udias *et al.* [6,24–26] and by Kelly [7]. Both calculations use the Coulomb gauge, the NLSH bound-state wave function [27], the energy dependent, atomic-mass independent parametrization for oxygen (EDAIO) optical potential of Cooper *et al.* [28], the cc2 current operator [29] (the use of cc1 yielded slightly poorer agreement with the data), and include the effects of electron distortion. We note that the NLSH wave function [27] yields values of binding and single-particle energies, as well as the charge radius for ^{16}O, which are in good agreement with data. Udias *et al.* solved the Dirac equation directly in configuration space, whereas Kelly solved a relativized Schrödinger equation and used the effective momentum approximation (EMA) to incorporate spinor distortion into an effective current operator based on that of Hedayati-Poor *et al.* [30]. Effectively, the primary difference between these two calculations is that Kelly used the EMA approximation for the lower components of the Dirac spinors while Udias *et al.* solved the Dirac equation directly. To remain consistent with the experimental data, the $1p_{3/2}$ state in both calculations includes an incoherent contribution from the positive-parity contaminants as parametrized by Leuschner *et al.* [11].

Figure 1 shows the cross section as a function of missing momentum at $E_{\mathrm{beam}} = 2.4$ GeV. The calculations of Udias *et al.* and Kelly are in very good agreement with the data. This agreement is attributed to the quality of the bound-state wave function used. The spectroscopic factors are 0.73 and 0.72 for the $1p_{1/2}$ state and 0.71 and 0.67 for the $1p_{3/2}$ state for the calculations of Udias *et al.* and Kelly, respectively.

We extracted A_{LT} from the measured cross sections (see Fig. 2). Note the large change in the slope of A_{LT} at $P_{\mathrm{miss}} \approx 300$ MeV$/c$. The data are compared to calculations by Udias *et al.* and Kelly. In all of Udias' calculations, the nucleon current is computed with a fully relativistic operator. The wave functions are four-component spinor solutions of the Dirac equation with scalar and vector potentials. As a result, their lower components are dynamically enhanced with respect to a solution of a Dirac equation without potentials (a free spinor). This dynamical effect of spinor distortions affects the A_{LT} and R_{LT} observables. To illustrate this point, we also present curves by Udias *et al.* in which this enhancement of the lower components is removed from the relativistic wave functions. Thus, the differences between the four Udias' curves demonstrate only the effect of spinor distortions. In these curves, all other ingredients are kept the same (in particular, the relativistic structure of the current operator and the upper components of the Dirac spinors). Note that the dotted-dashed curve (no spinor distortions) is essentially identical to one resulting from factorized calculations. As can be seen in the calculations of Udias *et al.* in Fig. 2, distortion of the bound-state spinors is more important than that of the ejectile spinors, although both are needed. Also presented in Fig. 2 are calculations by Kelly, which include spinor distortions. Kelly also sees an effect due to distortion of the bound-state spinors, but, because of the approximations he makes, his calculations are not as accurate for $P_{\mathrm{miss}} > 275$ MeV$/c$ [7].

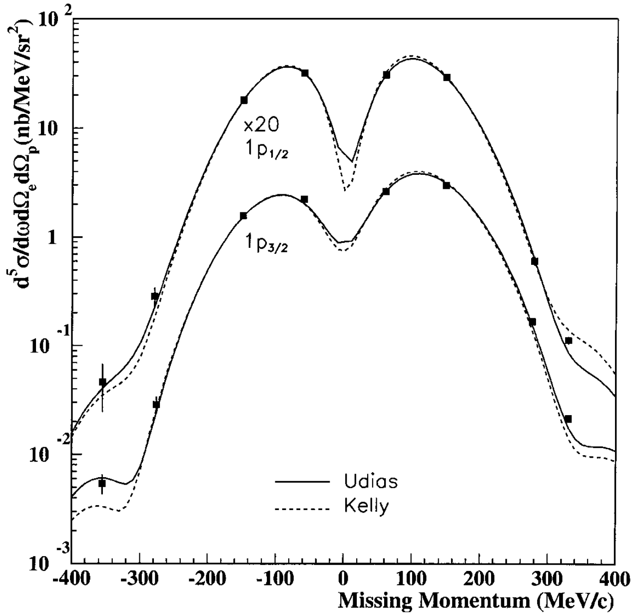

FIG. 1. Measured cross sections and DWIA calculations at $E_{\mathrm{beam}} = 2.4$ GeV. The solid line is the Udias *et al.* calculation [6,26] and the dashed line is the Kelly calculation [7]. The $1p_{1/2}$-state cross sections and calculations have been multiplied by a factor of 20.

We also extracted the response functions R_{L+TT}, R_{LT}, and R_T. Since we measured the cross sections in perpendicular kinematics, we could not isolate the longitudinal response function R_L. Instead, we extracted the combination $R_{L+TT} = R_L + \frac{V_{TT}}{V_L} R_{TT}$. Both Kelly and Udias calculate the term $\frac{V_{TT}}{V_L} R_{TT}$ to be small (<10%) for these kinematics. Figure 3 shows the response functions and calculations. Again, the calculations are in good agreement with the data. We note that spinor distortions are needed to reproduce R_{LT} in the missing momentum range $P_{\mathrm{miss}} < 275$ MeV$/c$ as well [6,26]. Hence, these relativistic dynamic effects are required to consistently reproduce both R_{LT} and A_{LT} over the entire measured P_{miss} range. Moreover, neither calculation includes any two-body currents, suggesting that such currents are unimportant at this Q^2. This suggestion is further supported by calculations which estimate the contribution of meson exchange and isobar currents in R_{LT} to be significant at lower Q^2 [31], but only

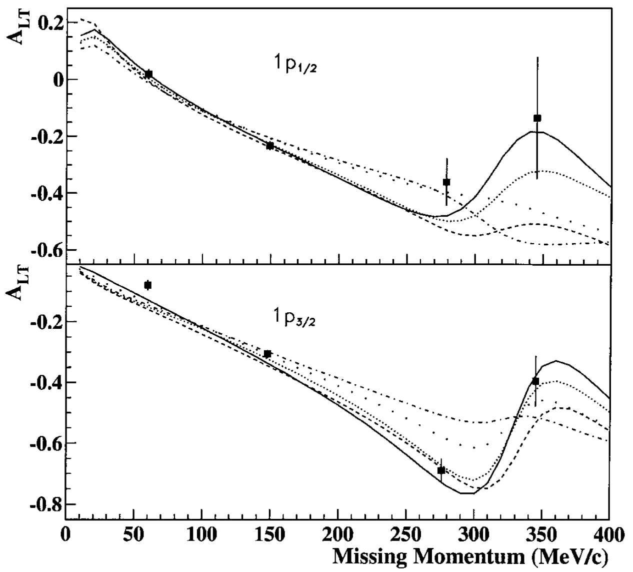

FIG. 2. Measured left-right asymmetry A_{LT} and DWIA calculations at $E_{\rm beam} = 2.4$ GeV. The dashed line is the Kelly calculation [7]. The other curves are from Udias *et al.* [6,26]. The solid line is the fully relativistic calculation. The densely dotted line is the calculation with only the bound-state spinor distortion included. The loosely dotted line is the calculation with only the scattered-state spinor distortion included. The dotted-dashed line is the calculation without spinor distortion included, which is essentially identical to factorized calculations. The error bars shown included both statistical and systematic uncertainties.

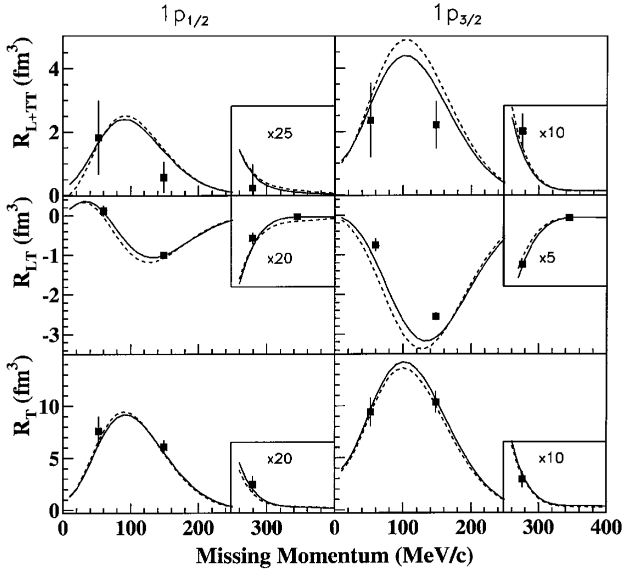

FIG. 3. Measured R_{L+TT}, R_{LT}, R_T, and DWIA calculations. The solid line is the Udias *et al.* calculation [6,26] and the dashed line is the Kelly calculation [7]. The data beyond 250 MeV/c missing momentum are expanded for clarity. The error bars shown include both statistical and systematic uncertainties.

approximately 2% and 8% for the $1p_{3/2}$ and $1p_{1/2}$ states, respectively, at this Q^2 [32].

In summary, we have measured ^{16}O$(e, e'p)$ $1p$-shell proton knockout in a previously inaccessible region of momentum transfer. These measurements included cross sections, the left-right asymmetry A_{LT}, and the response functions R_{L+TT}, R_{LT}, and R_T for missing momentum up to approximately 350 MeV/c. The cross section, asymmetry, and response functions are reproduced very well by modern relativistic DWIA calculations without the addition of any two-body currents. Structure in A_{LT} is observed at higher missing momentum which is consistent with predictions of relativistic calculations that include the dynamic enhancement of the lower components of Dirac spinors. This structure is not seen in the calculations if the enhancement of the lower components is removed.

We acknowledge the outstanding support of the staff of the Accelerator and Physics Divisions of Jefferson Laboratory that made this experiment successful. We thank Dr. T. W. Donnelly, Dr. J. M. Udias, and Dr. J. W. Van Orden for providing their theoretical calculations and for valuable discussions. We also thank Dr. J. M. Udias for providing us with the NLSH bound-state wave functions. This work was supported in part by the U.S. Department of Energy, the National Science Foundation, the Italian Istituto Nazionale di Fisica Nucleare (INFN), the French Atomic Energy Commission and National Center of Scientific Research, and the Natural Sciences and Engineering Research Council of Canada.

[1] S. Frullani and J. Mougey, Adv. Nucl. Phys. **14**, 1 (1984).

[2] J. J. Kelly, Adv. Nucl. Phys. **23**, 75 (1996); Phys. Rev. C **56**, 2672 (1997).

[3] The kinematical quantities are as follows: the scattered electron transfers momentum $\vec{q}$ and energy ω with $Q^2 = \vec{q}^{\,2} - \omega^2$. The ejected proton has mass m_p, momentum $\vec{p}_p$, energy E_p, and kinetic energy T_p. The cross section is typically measured as a function of missing energy $E_{\rm miss} = \omega - T_p - T_{\rm recoil}$ and missing momentum $\vec{P}_{\rm miss} = \vec{q} - \vec{p}_p$. The angle between the ejected proton and virtual photon is θ_{pq} and the azimuthal angle is ϕ. $\theta_{pq} > 0$ corresponds to $\phi = 180°$, $P_{\rm miss} > 0$, and $\theta_p > \theta_q$. $\theta_{pq} < 0$ corresponds to $\phi = 0°$.

[4] A. Picklesimer, J. W. Van Orden, and S. J. Wallace, Phys. Rev. C **32**, 1312 (1985).

[5] A. Picklesimer and J. W. Van Orden, Phys. Rev. C **40**, 290 (1989).

[6] J. M. Udias *et al.*, Phys. Rev. Lett. **83**, 5451 (1999).

[7] J. J. Kelly, Phys. Rev. C **60**, 044609 (1999); the calculations were revised using the NLSH wave functions.

[8] The cross section for $(e, e'p)$ can be written as $\frac{d^6\sigma}{d\Omega_e d\omega d\Omega_p dE_{\rm miss}} = \frac{E_p p_p}{(2\pi)^3}\sigma_{\rm Mott}(V_L R_L + V_T R_T + V_{LT} R_{LT} \times \cos\phi + V_{TT} R_{TT} \cos 2\phi)$, where the kinematic factors $\{V_i\}$ are known and the response functions $\{R_i\}$ contain information about the nuclear charge and current densities. One can extract response functions by measuring the cross section at fixed Q^2, ω, and θ_{pq} while varying the electron

scattering angle (which changes V_T) and ϕ. One can also extract the left-right asymmetry by measuring the cross section at $\phi = 0$, 180°: $A_{LT} = \frac{\sigma(\phi=0^\circ)-\sigma(\phi=180^\circ)}{\sigma(\phi=0^\circ)+\sigma(\phi=180^\circ)}$.

[9] L. Chinitz *et al.*, Phys. Rev. Lett. **67**, 568 (1991).

[10] M. Bernheim *et al.*, Nucl. Phys. **A375**, 381 (1982).

[11] M. Leuschner *et al.*, Phys. Rev. C **49**, 955 (1994).

[12] C. M. Spaltro *et al.*, Phys. Rev. C **48**, 2385 (1993).

[13] K. I. Blomqvist *et al.*, Phys. Lett. B **344**, 85 (1995).

[14] www.jlab.org/~fissum/e89003.html

[15] A. Saha, W. Bertozzi, R. W. Lourie, and L. B. Weinstein, Jefferson Laboratory Proposal 89-003, 1989; K. G. Fissum *et al.*, MIT-LNS Internal Report No. 02, 1997.

[16] www.jlab.org/Hall-A/equipment/HRS.html

[17] F. Garibaldi *et al.*, Nucl. Instrum. Methods Phys. Res., Sect. A **314**, 1 (1992).

[18] J. Gao, Ph.D. thesis, Massachusetts Institute of Technology, 1999 (unpublished).

[19] J. Gao *et al.*, MIT-LNS Internal Report No. 04, 1998.

[20] N. Liyanage *et al.*, MIT-LNS Internal Report No. 05, 1998.

[21] M. Liang, Jefferson Lab Technical Notes No. JLAB-TN-99029.

[22] G. G. Simon *et al.*, Nucl. Phys. **A333**, 381 (1980); L. E. Price *et al.*, Phys. Rev. D **4**, 45 (1971).

[23] E. Quint, Ph.D. thesis, University of Amsterdam, 1988 (unpublished); R. Florizone, Ph.D. thesis, Massachusetts Institute of Technology, 1999 (unpublished).

[24] J. M. Udias *et al.*, Phys. Rev. C **48**, 2731 (1993).

[25] J. M. Udias *et al.*, Phys. Rev. C **51**, 3246 (1995).

[26] J. M. Udias (private communication).

[27] M. M. Sharma, M. A. Nagarajan, and P. Ring, Phys. Lett. B **312**, 377 (1993).

[28] E. D. Cooper, S. Hama, B. C. Clark, and R. L. Mercer, Phys. Rev. C **47**, 297 (1993).

[29] T. de Forest, Jr., Nucl. Phys. **A392**, 232 (1983).

[30] M. Hedayati-Poor, J. I. Johansson, and H. S. Sherif, Phys. Rev. C **51**, 2044 (1995).

[31] J. E. Amaro *et al.*, Phys. Rev. C **60**, 014602 (1999).

[32] J. E. Amaro (private communication).